The Journal of Chemical Physics ARTICLE scitation.org/journal/jcp

Millimeter/sub-mm spectroscopy of the CrBr radical in the high spin $X^6\Sigma^+$ state

Cite as: J. Chem. Phys. 151, 194301 (2019); doi: 10.1063/1.5125013
Submitted: 20 August 2019 • Accepted: 28 October 2019 •
Published Online: 15 November 2019

T. J. Herman, J. P. Keogh, and L. M. Ziurys[a)]

AFFILIATIONS

Department of Chemistry and Biochemistry, Department of Astronomy, and Steward Observatory, University of Arizona, 1305 E. 4th Street, Tucson, Arizona 85719, USA

[a)]**Email:** lziurys@email.arizona.edu. **Telephone:** 520-626-0701. **Fax:** 520-621-5554.

ABSTRACT

The millimeter/submillimeter spectrum of the CrBr radical has been recorded in the frequency range of 220–300 GHz using direct absorption techniques, utilizing a new instrumental design. This study is the first spectroscopic investigation of this radical species by any method. CrBr was synthesized in a DC discharge by the reaction of chromium vapor, produced in a Broida-type oven, with Br_2CH_2 in argon. Six to nine rotational transitions were measured for four isotopologues of this molecule in their natural abundances, $^{52}Cr^{79}Br$, $^{52}Cr^{81}Br$, $^{53}Cr^{79}Br$, and $^{53}Cr^{81}Br$. Each transition was found to consist of six distinct fine structure components, indicating a $^6\Sigma^+$ ground electronic state, as observed for CrF and CrCl. Lines originating in the v = 1 and 2 vibrational states were recorded for $^{52}Cr^{79}Br$ and $^{52}Cr^{81}Br$ as well. The spectra were analyzed using a Hund's case (*b*) Hamiltonian, and rotational, spin-spin, and spin-rotation parameters were determined. The third-order spin-rotation constant γ_s and the fourth order spin-spin term θ were necessary for the analysis; these parameters are thought to play a role in states with high multiplicities. Equilibrium parameters were also derived for the CrBr; a bond length of r_e = 2.337 282 (30) Å and a vibrational constant of $\omega_e \cong 300$ cm^{-1} were determined. The sign and magnitude of the spin-spin and spin-rotation constants suggest the presence of nearby $^4\Pi$ and $^6\Pi$ excited states in CrBr, lying ~9000 cm^{-1} above the ground state. The new instrument design, employing more compact, free-space optics utilizing an offset ellipsoidal mirror, facilitated these measurements.

I. INTRODUCTION

Chromium halides have been of chemical interest for decades, particularly in organic synthesis. The chromium salts $CrCl_2$ and $CrCl_3$ have proven to be useful catalysts, enabling, for example, the cleavage and cross coupling of unactivated chemical bonds, such as C–O and C–N bonds, in conjunction with powerful Grignard reagents.[1] More recently, it has been shown that such salts, combined with alkyl halides, can lead to *ortho*-alkylated compounds by catalytic cleavage of unactivated C–H bonds at ambient temperature.[2] Another useful catalyst is $CrBr_3$, commonly employed in the polymerization of olefins.[3] Chromium halides also have some interesting structural properties.[4] The crystal arrangement of $CrBr_2$ appears to consist of Cr^{2+} ions surrounded by unusual distorted octahedra of bromine ions.[5] The 2D material, $CrBr_3$, is the first ferromagnetic semiconductor ever discovered.[6] It has been incorporated into van der Waals heterostructures with interesting tunneling properties, in particular when layered with graphene.[7]

Chromium and other diatomic transition metal halides have also been valuable in understanding basic chemical properties across the *d* electron rows. These molecules are thought to be best represented as M^+X^-,[8] with the unpaired electrons chiefly residing on the metal. The resulting electronic states of MX species are therefore thought to resemble those of the atomic M^+ ion in the "supermultiplet" model.[9] In this scenario, the electronic states of hydride MH species should be very similar to the MX series, but often there are differences. The ground electronic state of NiH is $^2\Delta_i$, for example, while those for NiF, NiCl, and NiBr are $^2\Pi_i$.[8] In the case of chromium, on the other hand, the hydride, fluoride, and chloride all have $^6\Sigma$ ground electronic states.[10–14]

One chromium halide species of interest is CrBr. Not only is it next in the halide series after CrF and CrCl, the molecule is the fundamental unit for chromium-bromine complexes of synthetic and materials interest. Unlike the chloride and fluoride counterparts, very little spectroscopic data or theoretical calculations exist for this radical, although mass spectrometric and matrix-isolation infrared studies on $CrBr_2$, $CrBr_3$, and $CrBr_4$ have been carried out.[15] In fact, the characterization of the 3*d*-bromide series is by no means complete, unlike the fluoride and chloride groups. Thus far, studies have been limited to microwave/millimeter-wave measurements of CuBr,[16,17] ScBr,[18] and NiBr,[19] as well as rotationally resolved optical work for the latter two species, and for TiBr.[20] It is therefore useful to spectroscopically investigate CrBr, to further the understanding of periodic trends in 3*d* bonding, and to provide benchmark data for applications to the larger chromium bromide systems, such as $CrBr_3$.

Here, we present the first spectroscopic study of the CrBr radical in its electronic ground state, conducted using millimeter/submillimeter direct absorption methods. This work is a continuation of an effort to characterize the complete 3*d* bromide series. Spectra from four isotopologues of this molecule were recorded in the v = 0 state ($^{52}Cr^{79}Br$, $^{52}Cr^{81}Br$, $^{53}Cr^{79}Br$, and $^{53}Cr^{81}Br$), and data were also obtained for the v = 1 and v = 2 states of $^{52}Cr^{79}Br$ and $^{52}Cr^{81}Br$. The appearance of six fine structure components per rotational transition for all species clearly identified the ground state as $^6\Sigma^+$. Here, we present our measurements and spectral analysis of CrBr, including derivation of the equilibrium parameters and interpretation of the spin-spin constants. We also compare this species with other chromium halides and across the 3*d*-bromine series.

II. EXPERIMENTAL

The pure rotational spectrum of CrBr ($X^6\Sigma^+$) was measured using the high-temperature millimeter-wave direct absorption spectrometer of the Ziurys group. The basic design of the instrument is described in detail elsewhere;[21,22] however, the spectrometer optics design has recently been enhanced, as shown in Fig. 1. These measurements are the first complete spectroscopic work using the new system. Briefly, the instrument consists of a radiation source, a reaction cell designed for high temperature chemistry, and a detector. Millimeter-wave radiation is produced by one of a suite of InP Gunn oscillators (WR-12, WR-10, and WR-8), phase-locked to a ~2 GHz synthesizer. Pairing the Gunn oscillators with one of a series of Schottky diode multipliers allows for nearly continuous frequency coverage from 65 to 850 GHz. The radiation is launched from the source by a scalar feed horn and propagated quasioptically through a polarizing grid and to an offset ellipsoidal mirror, where it is focused into the reaction cell. The mirror is the main new optics element (see Fig. 1). The radiation then passes into the cell through a z-cut quartz window, which replaced one made of Styrofoam-backed mylar. The new window has equivalent transmission as the previous one but is far more resistant to degradation by metal vapor. After one pass through the cell, the radiation reaches a beam waist[23] at a rooftop mirror, which reflects the radiation back through the cell with a 90° change in polarization. The radiation is then refocused by the ellipsoidal mirror onto the wire grid, which reflects it onto a lens and into the detector, an InSb hot electron bolometer (Fig. 1). Phase-sensitive detection is accomplished by FM modulation of the Gunn oscillator, with detection at 2*f*, producing second-derivative line shapes. The reaction cell is a double-walled, water-cooled steel chamber with an attached Broida-type oven and is specifically designed to vaporize high-temperature transition metals.

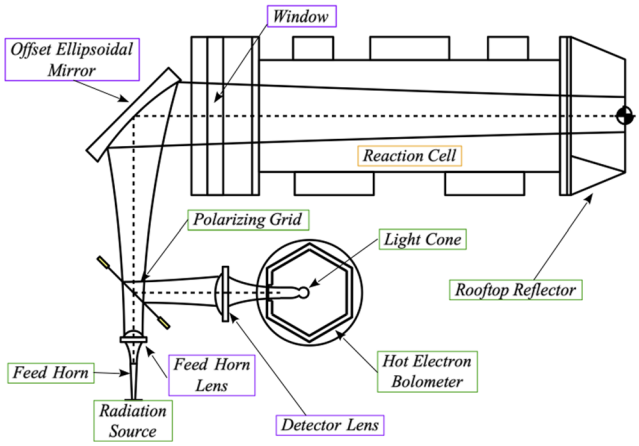

FIG. 1. New optics design for the high temperature spectrometer of the Ziurys group, showing the basic system layout and the $4\omega_0$ contour of the radiation as it propagates from source to detector. The radiation is launched from the source by a feed horn/lens combination and focused to a waist at the polarizing grid. The beam diverges to the offset ellipsoidal mirror, which focuses it through a z-cut quartz window and into the reaction cell to a waist at the rooftop reflector, located at the back of the chamber. This rooftop mirror then reflects the radiation back through the cell with a 90° change in polarization, where it is refocused by the ellipsoidal mirror to a waist at the grid. From this point, the beam reflects off the grid and into the InSb bolometer detector through a lens. The use of the ellipsoidal mirror replaced several other optic elements, shortening the radiation path and greatly reducing baseline ripple. For more details on the mirror and overall optics design, see Ref. 24.

Implementation of the offset ellipsoidal mirror greatly simplified the previous optics, replacing two spherical mirrors and a path length modulator (see Refs. 22 and 24). The new mirror maintains the beam waist at the rooftop reflector but shortens the overall radiation path length by a factor of 3.2. Direct absorption spectrometers at millimeter wavelengths typically suffer from nonlinear baselines. Use of streamlined Gaussian-beam optics helps to prevent needless reflections from reaction cell walls and other spectrometer elements but cannot eliminate the basic electrical mismatch between the coherent radiation source and the broadband InSb bolometer. The main source of nonlinear baselines in our instruments is this mismatch, but the resulting standing wave can be managed if the effective path length L between the source and detector is minimized. The frequency of the standing wave, $\nu = c/2L$, is then increased, in the case of this spectrometer from ~16 MHz to ~50 MHz, such that only ~2 cycles occur within the typical scan range of 110 MHz, significantly reducing the baseline ripple. See Ref. 24 for further details.

The CrBr radical was produced in a DC glow discharge by the reaction of chromium vapor and dibromomethane, CH_2Br_2. The metal vapor, produced in a specially insulated Broida-type oven, was mixed with 1–2 mTorr of CH_2Br_2, introduced just above the oven assembly. Approximately 10 mTorr of argon carrier gas was flowed

from beneath the oven to entrain the chromium vapor. The optimal DC glow discharge required 160 mA at 270 V. The area between the alumina crucible containing the metal and the oven outer wall was insulated with old crucible pieces, and Zirconia felt was wrapped around the crucible heating element, offering additional insulation. Unlike in the production of titanium,[25] which required boron nitride crucibles, alumina crucibles proved effective for the metal vaporization. Production of chromium vapor in the discharge could be monitored by the appearance of a distinct rich blue luminescence, visible just above the oven.

Transition frequencies were recorded using 5 MHz wide scans, taken in pairs where one scan increased in frequency and one decreased in frequency, which were then averaged. Only one or two of these pairs were required for adequate signal to noise for the ground vibrational states of the ^{52}Cr isotopologues; for the higher vibrational states and for the ^{53}Cr isotopologues, 2–10 pairs were required. The spectral lines were fit with Gaussian profiles to determine the center frequencies. Linewidths typically ranged from 720 to 910 kHz over the scanned region of 220–300 GHz.

III. RESULTS

There was no prior theoretical or experimental work for CrBr. Therefore, a rotational constant was predicted by mass scaling from those of CrF and CrCl.[13,14] The value predicted for ^{52}Cr^{79}Br, the main isotopologue, was B ~ 3020 MHz. Based on this constant, a search for CrBr was conducted, recognizing that two abundant isotopes of both bromine (^{79}Br:^{81}Br = 50.7%:49.3%) and chromium (^{52}Cr:^{53}Cr = 83.8%:9.5%) exist.

For the initial search, the region of 255–290 GHz (~12 B) was scanned continuously with the goal of finding harmonic patterns in the data. A series of sextet patterns were soon located that repeated at ~2B throughout the 35 GHz region. The six features were composed of a somewhat unevenly spaced multiplet, with one component showing some broadening due to hyperfine interactions (see Fig. 2). It was then confirmed that the lines in question arose from both chromium and the bromine precursor. After optimizing production conditions, additional scanning was performed such that a total range of 220–300 GHz was searched. Patterns were then assigned to the four different isotopologues, ^{52}Cr^{79}Br, ^{52}Cr^{81}Br, ^{53}Cr^{79}Br, and ^{53}Cr^{81}Br, and the v = 1 and 2 vibrationally excited states of ^{52}Cr^{79}Br and ^{52}Cr^{81}Br were located. It became clear that the ground electronic state of CrBr is $^6\Sigma^+$.

In the end, a total of 342 individual lines were recorded for chromium bromide. At least six rotational transitions ($N' \leftarrow N''$), each consisting of six fine structure lines, were measured for each species, with additional transitions being measured in some cases. For ^{52}Cr^{79}Br, the main isotopologue, for its v = 0 and v = 1 states, eight and nine transitions were recorded each. Eight were recorded for the v = 0 state of ^{52}Cr^{81}Br, and seven for the v = 2 state of ^{52}Cr^{79}Br were measured. Note that the two bromine isotopes have nearly identical abundances. A subset of the measurements is shown in Table I. The complete dataset is available in the supplementary material.

Figure 2 shows the representative spectra of the $N = 40 \leftarrow 39$ and $N = 39 \leftarrow 38$ transitions of the ^{52}Cr^{79}Br (left) and ^{52}Cr^{81}Br (right) isotopologues, respectively, measured in natural bromine abundance. The six fine structure components in each transition, indicated by the pattern displayed under the spectra, are labeled by F_1, F_2, F_3, F_4, F_5, and F_6, where F_1 is $N = J - 5/2$, F_2 is $N = J - 3/2$, etc. The obvious sextet pattern confirms the electronic ground state of CrBr as $^6\Sigma^+$. As mentioned, the six fine structure lines do not

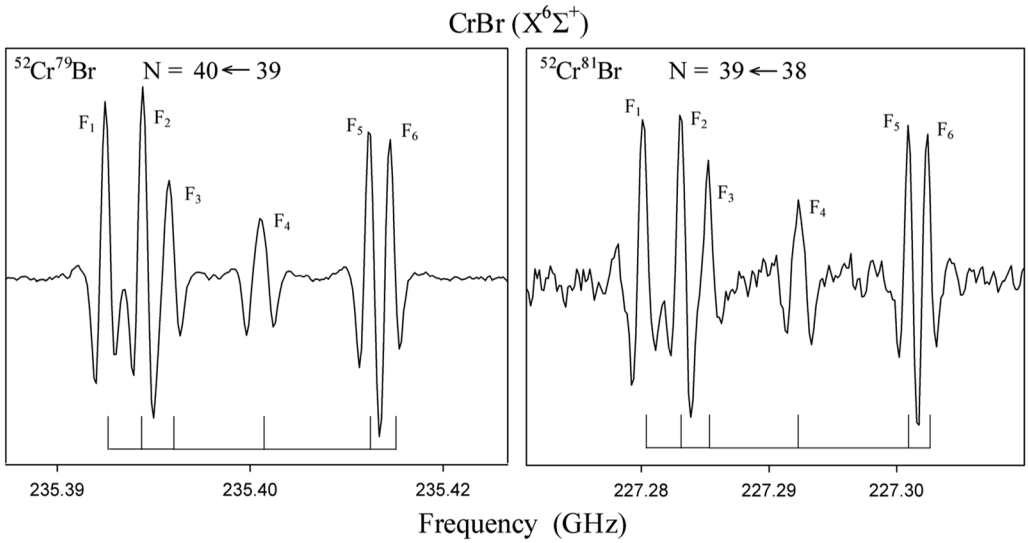

FIG. 2. Spectra of rotational transitions of the ^{52}Cr containing isotopologues of CrBr ($X^6\Sigma^+$). On the left is the $N = 40 \leftarrow 39$ transition of ^{52}Cr^{79}Br measured near 235.4 GHz; on the right is the $N = 39 \leftarrow 38$ transition of ^{52}Cr^{81}Br recorded near 227.3 GHz. The sextet fine structure pattern, labeled by F_1 through F_6, is clearly apparent in these data and is also indicated underneath the spectra. The fine structure pattern is clearly not symmetric but consistently repeats in both isotopologues. The F_4 component is slightly broadened by bromine hyperfine interactions, reducing its overall intensity. Each spectrum shows a continuous, ~40 MHz wide region, created from two 70 s, 110 MHz-wide scans.

TABLE I. Selected rotational transitions for CrBr ($X^6\Sigma^+$).[a]

		$^{52}Cr^{79}Br$		$^{52}Cr^{81}Br$		$^{53}Cr^{79}Br$		$^{53}Cr^{81}Br$	
$N' \leftarrow N''$	$J' \leftarrow J''$	ν_{obs}	$\nu_{obs-calc}$	ν_{obs}	$\nu_{obs-calc}$	ν_{obs}	$\nu_{obs-calc}$	ν_{obs}	$\nu_{obs-calc}$
41 ← 40	38.5 ← 37.5	241 262.074	0.047	238 903.824	−0.057				
	39.5 ← 38.5	241 264.913[b]	...	238 906.598	0.049				
	40.5 ← 39.5	241 266.793	−0.155	238 908.668	−0.192				
	41.5 ← 40.5	241 273.645	0.132	238 915.053	0.017				
	42.5 ← 41.5	241 281.953	−0.175	238 923.308	0.122				
	43.5 ← 42.5	241 283.667	−0.023	238 925.076	0.079				
46 ← 45	43.5 ← 42.5	270 585.299	−0.005	267 941.380	−0.125	267 511.710	0.067	264 867.645	−0.001
	44.5 ← 43.5	270 587.830	0.115	267 943.858[b]	...	267 514.061	0.074	264 870.048	0.156
	45.5 ← 44.5	270 589.798	0.283	267 945.864	−0.166	267 517.135[b]	...	264 872.083	−0.086
	46.5 ← 45.5	270 594.680	−0.149	267 950.526[b]	...	267 520.892	0.358	264 876.019	0.106
	47.5 ← 46.5	270 602.318	0.030	267 958.166	0.305	267 528.486	−0.273	264 884.216	−0.083
	48.5 ← 47.5	270 604.980	−0.033	267 960.743	0.135	267 530.986	−0.053	264 886.640	−0.056
47 ← 46	44.5 ← 43.5	276 445.824	0.050	273 744.858	−0.070	273 305.915	0.007	270 604.945	0.114
	45.5 ← 44.5	276 450.283[b]	...	273 747.308	−0.196	273 308.347	0.034	270 607.046	−0.116
	46.5 ← 45.5	276 448.314[b]	...	273 749.282	−0.001	273 310.349[b]	...	270 609.323	0.028
	47.5 ← 46.5	276 454.890	−0.129	273 753.556[b]	...	273 314.471	0.048	270 612.937	0.137
	48.5 ← 47.5	276 462.467	0.024	273 761.196	0.203	273 322.239	−0.104	270 620.787	−0.076
	49.5 ← 48.5	276 465.195	−0.157	273 763.919	0.046	273 324.973	0.075	270 623.515	0.032
50 ← 49	47.5 ← 46.5					290 679.971	−0.028	287 807.819	−0.014
	48.5 ← 47.5					290 682.323	0.002	287 810.175	0.007
	49.5 ← 48.5					290 684.296	0.075	287 812.070	0.055
	50.5 ← 49.5					290 687.361	−0.226	287 814.955	−0.186
	51.5 ← 50.5					290 695.114	0.170	287 822.677	0.084
	52.5 ← 51.5					290 698.235	−0.024	287 825.797	0.001

[a] In MHz.
[b] Blended lines, not included in the fit.

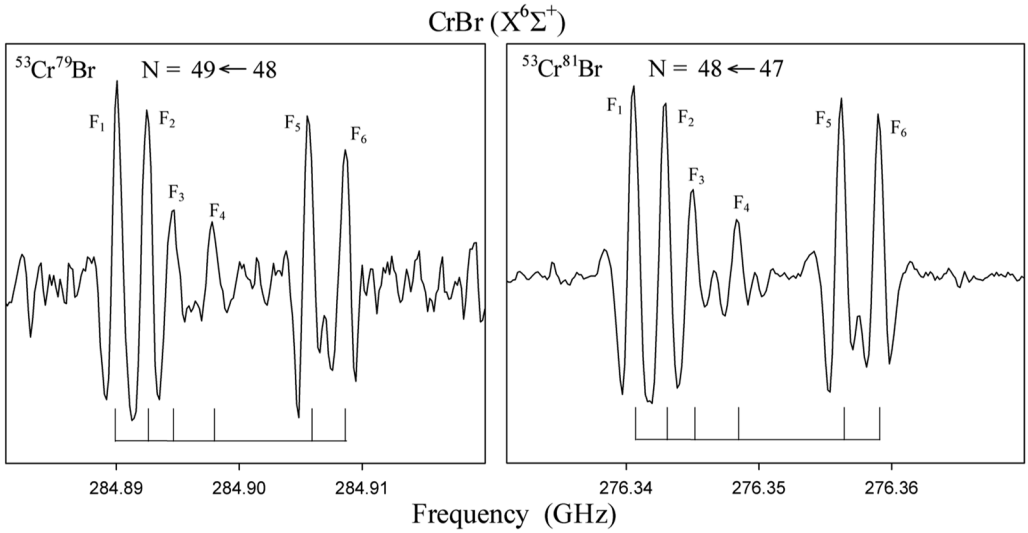

FIG. 3. Spectra of rotational transitions of the ^{53}Cr containing isotopologues of CrBr ($X^6\Sigma^+$). On the left is the $N = 49 \leftarrow 48$ transition of $^{53}Cr^{79}Br$ near 284.9 GHz; on the right is the $N = 48 \leftarrow 47$ transition of $^{53}Cr^{81}Br$ observed near 276.3 GHz. The sextet fine structure pattern, indicated by F_1 through F_6 and by lines under the spectra, is again obvious in these data. The asymmetric fine structure pattern repeats in the chromium-53 isotopologues as well, with the broadening of the F_4 component by bromine hyperfine interactions. Each spectrum displays a ~40 MHz wide region, created from two 70 s, 110 MHz-wide scans.

compose a symmetrical sextet, however, as seen, for example, in CrCCH.[26] Rather, the F_1, F_2, and F_3 components cluster together—sufficiently close such that the second derivative profiles influence the intensity of the F_3 feature.

Assignment of the F ordering was an iterative process. We initially attempted all possible permutations of F_1, F_2, etc., assignments of the fine structure for $^{52}Cr^{79}Br$, using the rms of the fit and uncertainties in the fitting parameters as a guide. In almost all cases, we found that the rms of the given fit was unacceptably large—often exceeding 1 GHz. Furthermore, the uncertainties on many of the spectroscopic parameters exceeded the values themselves. Therefore, almost all assignments except two could be discarded. The best fit in terms of rms and parameter uncertainties used sequential labeling of the fine structure from F_1 to F_6, as stated above. This ordering was also found for both CrF and CrCl. The alternative fit, which simply reversed the F_2 and F_3 components, generated a larger rms by >30 kHz and resulted in larger uncertainties to the constants. Based on the past results for CrCl and CrF, and the better rms, we chose the former fit.

Also of note is the F_4 component, set in the middle of the pattern, which is lower in intensity because of its broadened line profile, attributable to bromine hyperfine interactions. Both ^{79}Br and ^{81}Br have nuclear spins of $I = 3/2$, with very similar magnetic moments of 2.10 and 2.26 bohrs magnetons, respectively.[27] Therefore, the overall pattern repeats in both bromine species. The broadened line, however, was not found to split into individual hyperfine components for any observed transitions. Variation in the hyperfine interactions among fine structure components in Σ states is common, for example, in VO and VS.[28,29] Note that chlorine hyperfine interactions in CrCl were not observed in the millimeter spectra and could only be measured with higher resolution FTMW methods, which showed that the hyperfine constants were quite small (<20 MHz).[13]

Figure 3 displays the spectrum of the $N = 49 \leftarrow 48$ and $N = 48 \leftarrow 47$ transitions of the $^{53}Cr^{79}Br$ (left) and $^{53}Cr^{81}Br$ (right) isotopologues, measured in natural abundance. The fine structure components are indicated by lines underneath the spectrum and are labeled by F_1, etc. The asymmetrical sextet configuration is apparent in these data, as well, and the F_4 component is broader than the other lines. Note that the ^{53}Cr nucleus also has a nuclear spin of $I = 3/2$ like the bromine nuclei but has a much smaller magnetic moment of −0.47 bohr magnetons.[27] Because unpaired electrons reside on the chromium nucleus, Cr hyperfine interactions might be seen; however, any additional splitting was simply not observed, as was found for $^{53}CrCN$.[30]

IV. ANALYSIS

Each isotopologue and vibrational state (v = 0, 1, and 2), a total of eight different species, were analyzed individually with a least-squares analysis[31] using Hund's case (b) effective Hamiltonian. The complete Hamiltonian includes molecular rotation, spin-rotation interactions, and spin-spin coupling. The third order spin-rotation term, characterized by the constant γ_s,[32] and fourth order correction to the spin-spin interaction, θ,[10] were also considered in the analysis,

$$\widehat{H}_{eff} = \widehat{H}_{rot} + \widehat{H}_{sr} + \widehat{H}_{ss} + \widehat{H}_{sr}^{(3)} + \widehat{H}_{ss}^{(4)}. \quad (1)$$

The third-order spin-rotation and fourth order spin-spin corrections are nonvanishing for states of quartet and quintet multiplicity, respectively, or higher.[10,12,32] They are explicit in the derivation of the effective Hamiltonian for such high spin states (see Refs. 33 and 34). The expressions for the terms are as follows, using the tensor form of $\hat{H}_{sr}$:[10,32]

$$\widehat{H}_{sr}^{(3)} = \frac{10}{\sqrt{6}}\gamma_s \mathrm{T}^3\left(\boldsymbol{L}^2, \boldsymbol{N}\right) \cdot \mathrm{T}^3(\boldsymbol{S}, \boldsymbol{S}, \boldsymbol{S}), \quad (2)$$

$$\widehat{H}_{ss}^{(4)} = \frac{\theta}{12}\left(35\boldsymbol{S}_z^2 - 30\boldsymbol{S}^2\boldsymbol{S}_z^2 + 25\boldsymbol{S}_z^2 - 6\boldsymbol{S}^2 + 3\boldsymbol{S}^4\right). \quad (3)$$

The results of this analysis are presented in Table II (v = 0 data) and Table III (v = 1 and 2). As shown in Table II, the $^{52}Cr^{79}Br$ and $^{52}Cr^{81}Br$ data were successfully fit with rotational, spin-rotation, and spin-spin parameters, with an rms of 105 and 184 kHz, respectively. Attempts to determine any of the bromine magnetic hyperfine and quadrupole constants from the broadened F_4 component proved unsuccessful. On the other hand, the higher order spin-

TABLE II. Spectroscopic parameters for CrBr (v = 0).[a]

Parameter	$^{52}Cr^{79}Br$	$^{52}Cr^{81}Br$	$^{53}Cr^{79}Br$	$^{53}Cr^{81}Br$
B	2946.645 3(70)	2917.794 4(88)	2913.105(14)	2884.256 8(79)
D	0.001 2742(18)	0.001 2478(20)	0.001 2432(29)	0.001 2180(17)
γ	−8.80(68)	−8.1(1.2)	−9.1(1.3)	−9.61(74)
γ_D	0.000 960(77)	0.000 88(12)	0.000 80(13)	0.000 834(72)
λ	−3047(87)	−2930(169)	−3443(192)	−3481(104)
λ_D	0.017 1(27)	0.014 0(37)	0.014 4(56)	0.011 9(34)
$\lambda_H \times 10^6$	−3.47(66)	−2.69(79)	−2.6(1.2)	−2.06(70)
γ_s	−1.596(90)	−1.52(18)	−1.45(14)	−1.501(79)
γ_{sD}	0.000 129(13)	0.000 120(19)	0.000 090(18)	0.000 096(10)
θ	−13.2(7.7)	−12(12)	35(16)	41.3(7.9)
rms	0.105	0.184	0.142	0.081
r (Å)	2.339 964(15)	2.339 953(14)	2.339 952(29)	2.339 939(27)

[a]Parameters in MHz, stated uncertainties are 3σ.

TABLE III. Spectroscopic parameters for CrBr (v = 1, 2).[a]

Parameter	$^{52}Cr^{79}Br$: v = 1	$^{52}Cr^{81}Br$: v = 1	$^{52}Cr^{79}Br$: v = 2	$^{52}Cr^{81}Br$: v = 2
B	2933.087 4(58)	2904.414(16)	2919.553(10)	2891.101(13)
D	0.001 2763(15)	0.001 2449(32)	0.001 2752(22)	0.001 2495(28)
γ	−8.34(70)	−8.6(1.7)	−8.7(1.1)	−8.2(1.3)
γ_D	0.000 919(73)	0.000 78(16)	0.000 81(11)	0.000 73(13)
λ	−299 4(96)	−3317(247)	−3344(158)	−3308(187)
λ_D	0.016 4(24)	0.011 0(11)	0.014 7(44)	0.011 2(56)
$\lambda_H \times 10^6$	−3.36(58)	−1.95[b]	−2.71(91)	−2.0(1.1)
γ_s	−1.612(86)	−1.46(19)	−1.58(12)	−1.51(14)
γ_{sD}	0.000 136(11)	0.000 092(21)	0.000 111(15)	0.000 101(18)
θ	−11.9(8.5)			
rms	0.129	0.231	0.147	0.146
r (Å)	2.345 366(14)	2.345 335(44)	2.350 796(25)	2.350 730(29)

[a]Parameters in MHz, stated uncertainties are 3σ.
[b]Held constant.

rotation and spin-spin terms, γ_s and θ, were essential for a good fit and were defined to within 3σ. Setting $\gamma_s = 0$, for example, increased the rms by a factor of >6. Also, various higher-order centrifugal distortion parameters were needed, such as λ_D, λ_H, γ_D, and γ_{sD}. These higher order terms are not unusual for high spin radicals containing transition metals (see Refs. 13, 14, 30, and 35); they in part account for small perturbations of nearby excited states, as discussed in Sec. V. The data for $^{53}Cr^{79}Br$ and $^{53}Cr^{81}Br$ were successfully analyzed with the same set of parameters, with rms values of 142 and 81 kHz, respectively. The θ term was small and positive for these isotopologues, in contrast to $^{52}Cr^{79}Br$ and $^{52}Cr^{81}Br$, where the parameter was small and negative. The ^{53}Cr isotopologues also had a more negative value for λ relative to the main chromium species. The constants λ and θ are highly correlated, however. The differences between these constants for the two sets of isotopologues likely reflect this correlation and the decreased signal-to-noise in the 53-chromium datasets.

The v = 1 and v = 2 states for $^{52}Cr^{79}Br$ and $^{52}Cr^{81}Br$ were analyzed almost identically to the v = 0 data (see Table III), with rms of the fits in the range of 81–184 kHz. However, θ could only be fit for the v = 1 dataset for the main isotopologue; otherwise, it was undefined. Also, λ_H had to be fixed in the analysis for v = 1 lines of $^{52}Cr^{81}Br$, which had fewer transitions measured than most other species.

From the vibrational data, equilibrium parameters B_e, D_e, and γ_e, as well as the rotation-vibration coupling parameter α_e, were also determined from a least squares analysis. Expressions for these constants are given in Ref. 36. From the equilibrium parameters, the fundamental vibrational frequency ω_e was estimated, using the Kratzer relationship,[37]

$$\omega_e \cong \sqrt{\frac{4B_e^3}{D_e}}. \tag{4}$$

From ω_e, α_e, and B_e, the anharmonicity constant $\omega_e\chi_e$ can be calculated using the expression of Pekeris[38] and then the dissociation energy, D_E. The values of these parameters, as well as the equilibrium bond length, r_e, are listed in Table IV for both ^{52}Cr isotopologues.

TABLE IV. Equilibrium parameters for CrBr.[a]

Parameter	$^{52}Cr^{79}Br$	$^{52}Cr^{81}Br$
B_e	2953.414(35)	2924.457(99)
α_e	13.546(21)	13.347(58)
D_e	0.001 2745(46)	0.001 241(11)
γ_e	−8.7(1.2)	−8.3(1.3)
r_e (Å)	2.337 281(28)	2.337 286(80)
ω_e (cm^{-1})	299.93(54)	298.9(1.3)
$\omega_e x_e$ (cm^{-1})	1.090 7(28)	1.082 0(67)
D_E (eV)	2.557(11)	2.559(28)

[a]Parameters in MHz unless specified otherwise, uncertainties are 3σ.

V. DISCUSSION

This study has clearly demonstrated that the electronic ground state of the CrBr radical is $^6\Sigma^+$, as found for CrF and CrCl,[13] as indicated by the fine structure pattern. In analogy to the other halides, the valence electron configuration of CrBr is $13\sigma^1 1\delta^2 6\pi^2$. The 1δ orbital is nonbonding, created from the 3dδ atomic orbital, and is located on the chromium nucleus. The 6π orbital is principally 3dπ in character, with some minor contributions from the chromium 4*p* and bromine 4*p* orbitals. Similarly, the 13σ orbital is chiefly chromium 4*s* and $3d_{zz}$ in composition (sd_{zz} hybridized) but includes small amounts of bromine 4*s* and $4p_z$ character.[39] This orbital composition is consistent with the lack of observed bromine hyperfine structure. The unpaired electrons, for the most part, are located on the chromium nucleus.

From the equilibrium rotational constant, the equilibrium bond length for CrBr is established to be 2.337 281(28) Å. This value

is larger than that of CrCl (2.193 78(1) Å),[14] as might be expected, as the atomic radius of bromine is 1.15 Å compared to 1.00 Å for chlorine. The bond length for chromium bromide is shorter than the "short" Cr–Br bond distance of 2.545 ± 0.01 Å determined for the crystal structure of $CrBr_2$ by X-ray diffraction.[5] The "long" bond length from crystallography is 2.998 ± 0.01 Å.

The vibrational constants estimated for CrBr (see Table IV) are $\omega_e \cong 300\ cm^{-1}$ and $\omega_e\chi_e \cong 1.09\ cm^{-1}$. There are no other experimental or theoretical values for CrBr for comparison. However, these constants are consistent with those for other 3*d* bromides, including ScBr ($\omega_e \cong 339\ cm^{-1}$ and $\omega_e\chi_e \cong 1.1\ cm^{-1}$),[18] NiBr ($\omega_e \cong 330\ cm^{-1}$),[19] and ZnBr $\omega_e \cong (285\ cm^{-1}$, $\omega_e\chi_e \cong 1.04\ cm^{-1}$).[36] The vibrational constant for CrBr follows the trend of decreasing frequency with heavier molecular mass, as is expected. The vibrational constants here should aid in further studies of CrBr at other wavelengths.

These measurements of CrBr provide additional insight into bond length trends across the 3*d* series. As shown in Fig. 4, the bond distances of the 3*d* chlorides qualitatively follow a "double hump" pattern that has been theoretically predicted for the diatomic 3*d* oxides and sulfides.[40] The pattern for the oxides and sulfides has been confirmed experimentally (e.g., Ref. 29); differences do exist between the two sets of species for cobalt and nickel[41] which cannot be interpreted in terms of simply filling bonding, nonbonding, and antibonding orbitals with *d* electrons. Therefore, it is interesting to compare the 3*d* bromide series to their chloride analogs. Unfortunately, experimental data exist for only half of the 3*d* bromide species, as shown in Fig. 4. The work done here for CrBr adds a new point in the plot. For the bromides, the bond length does show a ~0.05 Å decrease from titanium to chromium that is almost identical in the chlorides, which can be explained by the addition of electrons to bonding orbitals. Other common trends include an increase in bond distances from scandium to titanium and from copper to zinc. Thus far, the only significant deviation occurs from nickel to copper, where the bond length slightly increases for the chloride but decreases for the bromides. It is also interesting to note that the electronic ground states, also plotted for each 3*d* species, are thus far identical for these two halide series.

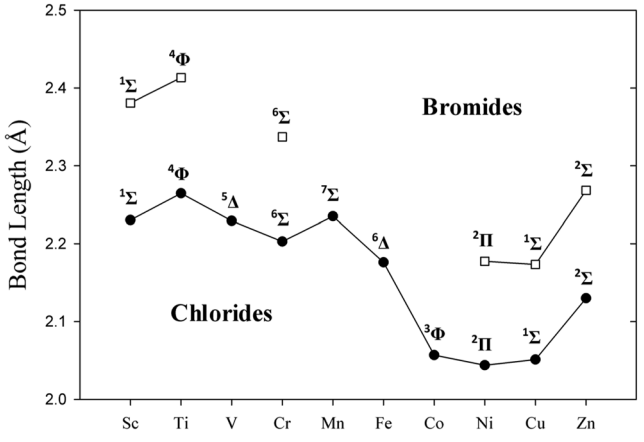

FIG. 4. A plot of the bond lengths and ground electronic states as a function of 3*d* metals for the chloride and bromide series. Bond lengths are typically r_e, except in the cases where only r_0 values are available (VCl, FeCl, NiCl, and NiBr). Experimental bond lengths are available for all chlorides, but not for the bromides. Nevertheless, the "double-hump" (Ref. 37) bond length trend established by the chlorides appears thus far to be duplicated in the bromides, with a small deviation between nickel and copper. The addition of CrBr to the plot shows that the bond length decreases from titanium to chromium significantly in both halide series.

A summary of the spin parameters for CrF, CrCl, and CrBr is given in Table V. As shown in this table, the spin-spin parameter λ for CrBr is small (−3047 MHz) and negative, in contrast to CrF (16 157 MHz) and CrCl (7989 MHz), for which the terms are larger and positive.[13] In heavy transition metal compounds, the main contribution to the spin-spin constant is second-order spin-orbit coupling, which connects the ground state to nearby excited states via the one-electron spin-orbit operator, $\hat{H}_{so} = \sum_i a_i \hat{l}_i \hat{s}_i$.[42] The spin-orbit operator links the states via the selection rules $\Delta S = 0, \pm 1$, $\Delta\Omega = 0$, and $\Delta\Sigma = -\Delta\Lambda = 0, \mp 1$. As observed for CrF, CrCl, and CrCN, the lowest lying quartet and sextet states are $^4\Pi$ and $^6\Pi$ states, respectively.[30,39] Note that there may also be low-lying $^4\Sigma^+$ and $^6\Sigma^+$ states, but they will not interact with the ground state because of the selection rule $\Sigma^+ \leftrightarrow \Sigma^-$.[43] The $^4\Pi$ and $^6\Pi$ states are thus likely to be the main contributors to λ and are responsible for its negative value. However, little is known concerning the excited states of CrBr.

On the other hand, the spin-spin constant does give insight into the nature of these two excited states. For a $^6\Sigma^+$ term, $|\Omega| = 5/2$, 3/2, and 1/2. The connection to the ground state for the $^4\Pi$ and $^6\Pi$ states occurs through their $|\Omega| = 5/2$, 3/2, and 1/2 components. As discussed by Flory *et al.*,[30] an evaluation of the perturbation-induced shift of the $\Sigma = 5/2$ substate relative to the $\Sigma = 3/2$ substate should give an indication of the respective contributions. Because $\langle S, \Sigma|H_{ss}|S,\Sigma\rangle = 2/3\ \lambda[3\Sigma^2 - S(S+1)]$, then $E_{\Sigma_{5/2}} - E_{\Sigma_{3/2}} = 8\lambda$. Using second-order perturbation theory, and considering only $^4\Pi$ and $^6\Pi$ contributors, then

$$8\lambda = E_{\Sigma_{5/2}} - E_{\Sigma_{3/2}} = \sum_{^4\Pi,^6\Pi} \left\{ \frac{\left|\langle \Pi_{5/2}|H_{so}|^6\Sigma_{5/2}\rangle\right|^2}{E_{\Sigma_{5/2}} - E'} - \frac{\left|\langle \Pi_{3/2}|H_{so}|^6\Sigma_{3/2}\rangle\right|^2}{E_{\Sigma_{3/2}} - E'} \right\}. \quad (5)$$

Assuming the spin-orbit constant $a = a(Cr^+{}_{3d}) = 224\ cm^{-1}$,[43] the relevant matrix elements can be calculated,

TABLE V. Comparison of fine structure parameters between chromium halides.[a]

Parameter	CrF[b]	$Cr^{35}Cl$[b]	$^{52}Cr^{79}Br$
γ	408.557(30)	65.580(13)	−8.80(68)
λ	16 157.49(75)	7989.42(24)	−3047(87)
θ	−4.80(81)	−3.245(30)	−13.2(7.7)
γ_s	−8.1(2.2)	−4.1(2.1)	−1.596(90)

[a]Parameters in MHz, stated uncertainties are 3σ.
[b]Reference 13.

$$\left|\left\langle {}^4\Pi_{5/2}|H_{so}|{}^6\textstyle\sum^+{}_{5/2}\right\rangle\right|^2 = (3/2)a^2 = 75\,260\ (\mathrm{cm}^{-1})^2,$$

$$\left|\left\langle {}^4\Pi_{3/2}|H_{so}|{}^6\textstyle\sum^+{}_{3/2}\right\rangle\right|^2 = (9/10)a^2 = 45\,160\ (\mathrm{cm}^{-1})^2,$$

$$\left|\left\langle {}^6\Pi_{5/2}|H_{so}|{}^6\textstyle\sum^+{}_{5/2}\right\rangle\right|^2 = (3/4)a^2 = 37\,632\ (\mathrm{cm}^{-1})^2,$$

$$\left|\left\langle {}^6\Pi_{3/2}|H_{so}|{}^6\textstyle\sum^+{}_{3/2}\right\rangle\right|^2 = (6/5)a^2 = 60\,025\ (\mathrm{cm}^{-1})^2.$$

Using Eq. (5) and the values above, and assuming $E_{\Sigma_{5/2}} \sim -E_{\Sigma_{3/2}}$, and $E_{^6\Pi} \sim E_{^4\Pi}$, as predicted for CrF and CrCl, the approximate energies of the Π perturbing states can be estimated. Note that the summation of the matrix elements above does lead to a negative spin-spin constant, as observed. This calculation suggests that the excited $^4\Pi$ and $^6\Pi$ states lie ~9400 cm^{-1} above the ground state for CrBr. In CrCl, they reside at energies ~11 500 cm^{-1} and 9000 cm^{-1} above the ground state, respectively,[39] consistent with those predicted for CrBr.

For CrBr, the spin-rotation parameter, γ = −8.80 (68) MHz, is also negative. In contrast, those of CrF and CrCl are positive [408.557(30) MHz and 65.580(13) MHz; see Table V] with a significant decrease from the fluoride to the chloride—the same trend as for the spin-spin constant. Again, the main contribution to γ is second-order spin-orbit coupling from nearby excited states. The selection rules for this type of perturbation are $\Delta S = 0$, $\Delta\Lambda = \pm 1$,[43] suggesting that the main contributor is the nearby $^6\Pi$ state. Experimentally, the $^6\Pi$ state in CrCl lies near 9000 cm^{-1}, as mentioned, while theory predicts the $^4\Pi$ term to be at 11 000 cm^{-1}. This difference would suggest that the $^6\Pi$ state in CrBr lies at ~8100 cm^{-1}, recognizing that the calculated energy of ~9400 cm^{-1} assumes $E(^6\Pi) \sim E(^4\Pi)$, and the sextet state likely lies lower in energy. This result is consistent with the small, positive spin-rotation constant for CrCl, which then becomes small and negative for CrBr as the perturbing $^6\Pi$ state drops in energy.

The third order spin-rotation constant γ_s becomes increasingly positive in CrBr, in comparison with CrF and CrCl. For the bromide, γ_s = −1.596 (90) MHz, while the parameter is −4.1 (2.1) MHz in CrCl and −8.1(2.2) MHz in CrF.[13] The need for this constant is evident from the fit, which worsens by a factor of 8 in rms when excluded. For the fourth order spin-spin constant θ, the trend is not as clear. For chromium bromide, θ = −13.2(7.7) MHz, relative to that of CrF of −4.80(81) MHz and −3.245(30) MHz for CrCl.[13] The other trends suggest that θ might be positive for CrBr. The γ_s and θ terms arise from the third-rank and fourth-rank tensor operators $T^3(\boldsymbol{S}^3)$ and $T^4(\boldsymbol{S}^4)$, which couple the ground $^6\Sigma^+$ state with nearby excited states ($^6\Pi$, $^4\Pi$, $^4\Sigma^-$, etc.). The consistent trend for at least γ_s reflects the changing energies of these excited states in the halide series.

The "supermultiplet" model suggests that the electronic states of M^+X^- species should mimic those of the M^+ ion,[9] in this case Cr^+. This ion has a ^6S ground state with a d^5 electron configuration, and the first excited state is ^6D (sd^4). A low-lying ^4D state also exits (sd^4) for Cr^+. The first excited sd^4 electron configuration is thought to give rise to the excited $^6\Pi$ state in CrX species, as well as additional $^6\Sigma^+$ and $^6\Delta$ terms. The exact energy ordering is not known, especially for CrBr. The low-lying quartet state leads to $^4\Sigma$, $^4\Pi$, and $^4\Delta$ states,[39] whose relative energies are also subject to debate. In any event, the data presented here are consistent with the supermultiplet approximation, but clearly significant additional information concerning the excited states of CrBr is needed for a complete analysis within the context of this model.

VI. CONCLUSIONS

This work is the first spectroscopic study of the CrBr radical, added additional data to understanding the 3*d* bromide series across the periodic table and also down the CrX column. This work provides further evidence that bonding in the bromides follows that of the chlorides, as interpreted by bond lengths and ground state terms. It also shows that there is systematic change in the electronic manifold from CrF to CrBr, as evidenced by the spin parameters. These constants suggest the existence of nearby $^6\Pi$ and $^4\Pi$ excited states, consistent within the "supermultiplet" model. Finally, CrBr is one of a small number of $^6\Sigma$ states that have been studied at high spectral resolution, further testing the theory of open-shell molecules and the necessity of higher order spin terms.

SUPPLEMENTARY MATERIAL

See the supplementary material for a complete list of measured transitions.

ACKNOWLEDGMENTS

The authors would like to thank Mark Burton for helpful discussions. This research was supported by NSF (Grant No. CHE-1565765).

REFERENCES

[1] X. Cong, H. Tang, and X. Zeng, J. Am. Chem. Soc. **137**, 14367 (2015).
[2] J. Tang, P. Liu, and X. Zeng, Chem. Commun. **54**, 9325–9328 (2018).
[3] D. L. Perry, *Handbook of Inorganic Compounds*, 2nd ed. (CRC Press, 2011), Vol. 122.
[4] H. Wang, V. Eyert, and U. Schwingenschlögl, J. Phys.: Condens. Matter **23**, 116003 (2011).
[5] J. W. Tracy, N. W. Gregory, and E. C. Lingafelter, Acta Crystallogr. **15**, 672–674 (1962).
[6] T. Ichiro, J. Phys. Soc. Jpn. **15**, 1664–1668 (1960).
[7] D. Ghazaryan, M. T. Greenaway, Z. Wang, V. H. Guarochico-Moreira, I. J. Vera-Marun, J. Yin, Y. Liao, S. V. Morozov, O. Kristanovski, A. I. Lichtenstein, M. I. Katsnelson, F. Withers, A. Mishchenko, L. Eaves, A. K. Geim, K. S. Novoselov, and A. Misra, Nat. Electron. **1**, 344–349 (2018).
[8] E. D. Tenenbaum, M. A. Flory, R. L. Pulliam, and L. M. Ziurys, J. Mol. Spectrosc. **244**, 153–159 (2007).
[9] J. Gray, M. Li, T. Nelis, and R. Field, J. Chem. Phys. **95**, 7164–7178 (1991).
[10] S. M. Corkery, J. M. Brown, S. P. Beaton, and K. M. Evenson, J. Mol. Spectrosc. **149**, 257 (1991).
[11] D. T. Halfen and L. M. Ziurys, Astrophys. J. **611**, L65 (2004).
[12] J. J. Harrison, J. M. Brown, D. T. Halfen, and L. M. Ziurys, Astrophys. J. **637**, 1143 (2006).
[13] K. Katoh, T. Okabayashi, M. Tanimoto, Y. Sumiyoshi, and Y. Endo, J. Chem. Phys. **120**, 7927 (2004).
[14] T. Oike, T. Okabayashi, and M. Tanimoto, J. Chem. Phys. **109**, 3501 (1998).
[15] P. D. Gregory and J. S. Ogden, J. Chem. Soc., Dalton Trans. **1995**, 1423.

[16]R. J. Low, T. D. Varberg, J. P. Connelly, A. R. Auty, B. J. Howard, and J. M. Brown, J. Mol. Spectrosc. **161**, 499 (1993).
[17]X. Wang, L. Wang, R. Brown, P. Schwerdtfeger, D. Schröder, and H. Schwarz, J. Chem. Phys. **114**, 7388–7395 (2001).
[18]W. Lin, S. A. Beaton, C. J. Evans, and M. C. L. Gerry, J. Mol. Spectrosc. **199**, 275 (2000).
[19]E. Yamazaki, T. Okabayashi, and M. Tanimoto, J. Chem. Phys. **121**, 162 (2004).
[20]A. G. Adam, W. S. Hopkins, W. Sha, and D. W. Tokaryk, J. Mol. Spectrosc. **236**, 42 (2006).
[21]L. M. Ziurys, W. L. Barclay, M. A. Anderson, D. A. Fletcher, and J. W. Lamb, Rev. Sci. Instrum. **65**, 1517 (1994).
[22]P. M. Sheridan, S. K. McLamarrah, and L. M. Ziurys, J. Chem. Phys. **119**, 9496 (2003).
[23]P. F. Goldsmith, *Quasioptical Systems: Gaussian Beam Quasioptical Propagation and Applications* (IEEE Press, New Jersey, 1998).
[24]J. P. Keogh, "Instrumental advances and applications in millimeter/submillimeter-wave spectroscopy," Ph.D. dissertation (University of Arizona, 2018).
[25]A. P. Lincowski, D. T. Halfen, and L. M. Ziurys, Astrophys. J. **833**, 9 (2016).
[26]J. Min and L. M. Ziurys, J. Chem. Phys. **144**, 184308 (2016).
[27]C. H. Townes and A. L. Schawlow, *Microwave Spectroscopy* (Dover Publications, New York, 1975).
[28]M. A. Flory and L. M. Ziurys, J. Mol. Spectrosc. **247**, 76–84 (2008).
[29]G. R. Adande and L. M. Ziurys, J. Mol. Spectrosc. **290**, 42–47 (2013).
[30]M. A. Flory, R. W. Field, and L. M. Ziurys, Mol. Phys. **105**, 585–597 (2007).
[31]J. M. Brown, private communication (2006).
[32]T. Nelis, J. M. Brown, and K. M. Evenson, J. Chem. Phys. **92**, 4067–4076 (1989).
[33]J. T. Hougen, Can. J. Phys. **40**(5), 598–606 (1962).
[34]J. M. Brown and D. J. Milton, Mol. Phys. **31**, 409–422 (1976).
[35]D. T. Halfen and L. M. Ziurys, Chem. Phys. Lett. **496**, 8–13 (2010).
[36]M. A. Burton and L. M. Ziurys, J. Chem. Phys. **150**, 034303 (2019).
[37]W. Gordy and R. L. Cook, *Microwave Molecular Spectra* (Wiley, New York, 1984).
[38]C. L. Pekeris, Phys. Rev. **45**, 98 (1934).
[39]J. F. Harrison and J. H. Hutchison, Mol. Phys. **97**, 1009–1027 (1999).
[40]A. J. Bridgeman and J. Rothery, J. Chem. Soc. Dalton Trans. **2000**, 211–218.
[41]M. A. Flory, S. K. McLamarrah, and L. M. Ziurys, J. Chem. Phys. **123**, 164312 (2005).
[42]J. Brown and A. Carrington, *Rotational Spectroscopy of Diatomic Molecules* (Cambridge University Press, United Kingdom, 2003).
[43]R. W. Field and H. Lefebvre-Brion, *The Spectra and Dynamics of Diatomic Molecules* (Elsevier, 2004).